Influence of the substrate bands on the *sp*-levels topology of Ag films on Ge(111)

P. Moras,[1] D. Topwal,[2] P. M. Sheverdyaeva,[3] L. Ferrari,[4] J. Fujii,[5] G. Bihlmayer,[6] S. Blügel,[6] and C. Carbone[1]

[1]*Istituto di Struttura della Materia, Consiglio Nazionale delle Ricerche, Trieste, Italy*
[2]*International Center for Theoretical Physics (ICTP), I-34014 Trieste, Italy*
[3]*Sincrotrone Trieste S.C.p.A., Area Science Park, SS 14, Km 163.5, I-34012 Trieste, Italy*
[4]*Istituto dei Sistemi Complessi, Consiglio Nazionale delle Ricerche, Roma, Italy*
[5]*TASC-INFM, Consiglio Nazionale delle Ricerche, Trieste, Italy*
[6]*Institut für Festkörperforschung and Institute for Advanced Simulation, Forschungszentrum Jülich, D-52425 Jülich, Germany*

Angle-resolved photoemission spectroscopy and first-principles calculations were employed to analyze unusual features in the electronic structure of ultrathin Ag films grown on Ge(111). The Ag *sp*-derived quantum well states exhibit hexagonal-like constant energy contours with different in-plane orientations near the center of the surface Brillouin zone, in striking contrast to the expectations for a free-standing Ag(111) layer. The experimental observations are explained by taking into account the effects of hybridization of the Ag states with the star-like shaped Ge band edges on constant energy planes.

PACS number(s): 73.21.Fg, 79.60.Dp

Surfaces and interfaces of ultrathin metallic films can behave as the reflecting walls of a two-dimensional quantum well, in analogy to the particle-in-a-box picture, and give rise to series of discrete quantum well (QW) electronic states.[1] The degree of localization of these energy levels within the metal layer is defined by their hybridization with the substrate wave functions. Film states coupled to substrate states of corresponding energy, symmetry, and spin propagate, partially or totally, across the interface plane. Truly confined QW states, instead, form in absence of such conditions. Besides the fundamental interest of these issues, the dualism between itinerant (three-dimensional) and localized (two-dimensional) electron behavior introduces in thin film structures functional properties with deep technological impact. The interlayer exchange coupling, for instance, originates from the spin-selective formation of QW states within a nonmagnetic spacer embedded between magnetic layers.[2]

Angle-resolved photoemission experiments on simple and noble metal layers exemplarily highlight the effects of hybridization on an *sp*-electronic band structure. The parabolic dispersion of the QW states appears to be abruptly interrupted by multiple discontinuities in films of Al on Si(111),[3] Mg on W(110),[4,5] and Mo(110),[5] and Ag on elemental semiconductors.[6–8] In Cu films on Co(001) the *sp*-levels bifurcate at characteristic positions in the energy-momentum space.[9] In Ag films on W(110) the spectral weight of the quasiparticle peak varies discontinuously as a function of the emission angle.[10] All these features contrast with the ground-state electronic structure of the metal layers and are explained in terms of symmetry-selective hybridization between film and substrate states.

In recent years several photoemission studies were devoted to the analysis of Ag films grown on Ge(111), which show an unexpectedly complex electronic structure. In these systems the *sp*-derived QW states display several gap openings. The breaks observed along the $\bar{\Gamma}$-$\bar{K}$ axis were interpreted as peculiar effects of hybridization, which manifest at the topmost band edges of the substrate material.[7] For the thinnest layers the interaction with the Ge electronic struc-

ture splits up the Ag(111) Shockley surface state in multiple subbands with nonparabolic dispersion.[11] Close to the Ag zone boundaries the experiments revealed also energy bands with bottoms located at the $\bar{M}$ points of Ge [the ratio of the in-plane lattice parameters of Ag(111) and Ge(111) is about 3:4]. These features were found to derive from the interference between the original QW states and their umklapp replicas, shifted by an in-plane wave vector defined by the substrate periodicity.[12,13] Model calculations could reproduce in detail the interference patterns generated on constant energy planes in proximity of the $\bar{M}_{\mathrm{Ge}}$ points.[13,14]

The present angle-resolved photoemission investigation examines, through full three-dimensional band mapping, characteristic features in the electronic structure of Ag films grown on Ge(111). Near the $\bar{\Gamma}$ point of the two-dimensional momentum space the QW states exhibit hexagonal-like constant energy contours, whose in-plane orientation changes as a function of energy and wave vector. First-principle calculations demonstrate that the observed shape evolution reflects symmetry and topology of the substrate band edges, across which the degree of hybridization between Ag and Ge states varies abruptly, rather than the behavior of a freestanding Ag(111) layer.

The experiments were performed at the VUV-Photoemission beamline on the Elettra synchrotron radiation laboratory. The substrates were *p*-doped Ge(111) wafers, whose surface was treated with cycles of Ar ion sputtering and annealing in order to show a sharp $c(2 \times 8)$ low-energy electron diffraction pattern. Ag layers, whose thickness is expressed throughout the paper in terms of monolayers (1 ML=2.36 Å), were deposited on the substrates held at 140 K and successively warmed up to room temperature, to favor the formation of atomically flat films.[15] The analysis of the electronic structure was performed at room temperature at a photon energy of 45 eV, using a Scienta R-4000 electron analyzer. The total energy and angular resolution were set to 15 meV and 0.3°, respectively. The constant energy cuts were constructed from sets of photoemission intensity maps acquired within an azimuthal sector of 60° covering the

angle between subsequent $\bar{\Gamma}$-$\bar{M}$ surface directions. First-principles calculations for the electronic structure of a Ag film and Ge bulk crystal were performed using density-functional theory in the local density approximation (LDA). We employed the full-potential augmented plane wave method[16] as implemented in the FLEUR code.[17] The experimental lattice constants were used and for Ge spin-orbit coupling was included in the calculations in a self-consistent manner.[18] The fundamental band gap of Ge was corrected to the experimental value using an LDA+U approach in a manner described in Ref. 19.

Figure 1 presents the results of *ab initio* calculations for the band structure of a free-standing 13 ML Ag film over a wide energy range. The *sp*-derived QW states in the proximity of the Fermi level (E_F) can be labeled with the main quantum number n, following the nomenclature usually adopted in the literature for (111)-oriented noble metal layers.[1] The $n=1$ and 2 bands as well as the Shockley surface state (SS), are nearly isotropic about the center of the surface Brillouin zone. States with a higher n, instead, exhibit less pronounced energy dispersion along $\bar{\Gamma}$-$\bar{M}$ than along $\bar{\Gamma}$-$\bar{K}$, because of the gap openings occurring at the $\bar{M}$ point (Ag zone boundary). On the Fermi surface [Fig. 1(b)] these differences result in a change in shape for the QW states as a function of the distance from the $\bar{\Gamma}$ point. The energy contours are almost perfectly circular inside an area with radius of 0.6 Å^{-1} centered about $\bar{\Gamma}$. At larger in-plane wave vectors, instead, they have an hexagonal-like aspect with corners lying on the $\bar{\Gamma}$-$\bar{M}$ axes and more pronounced anisotropy as the zone boundaries are approached. Calculations performed at deeper energies confirm the above outlined trend for the QW contours, as shown in Fig. 1(c) for the states at 1 eV below E_F.

Figure 2 reports the experimentally obtained constant energy cuts through the electronic structure of a 17 ML Ag film grown on Ge(111). In this system multiple ovals surround the $\bar{M}$ points of the Ge(111) surface Brillouin zone.[14] These ovals perturb the QW bands originating from the zone center in a limited portion of the two-dimensional momentum space, which approximately corresponds to a rim of radii comprised between 0.6 and 1.2 Å^{-1} at E_F [Fig. 2(a)]. The following analysis of the QW band patterns will be limited to a circular area of radius 0.6 Å^{-1} centered about the $\bar{\Gamma}$ point, where the perturbation is negligibly small.

The sequence of images in Fig. 2 shows the evolution of the QW states at selected energies. The behavior of the $n=3$ state appears to be unexpectedly complex, if compared to the calculations reported in Fig. 1. In panel (c) of Fig. 2 the state clearly exhibits an hexagonal-like energy contour with corners lying on the $\bar{\Gamma}$-$\bar{M}$ axes of the Ag(111) surface Brillouin zone. This azimuthal anisotropy tends to fade while moving toward E_F, but is still visible on the Fermi surface [panel (a)], where the QW state is totally confined within the film by the fundamental gap of Ge. On the other hand, the $n=3$ contour is almost circular in panel (d), as one would expect in proximity of the zone center in absence of perturbations. Surprisingly, in panel (e) the QW state forms again an hexagonal-like pattern, rotated in-plane by 30° with re-
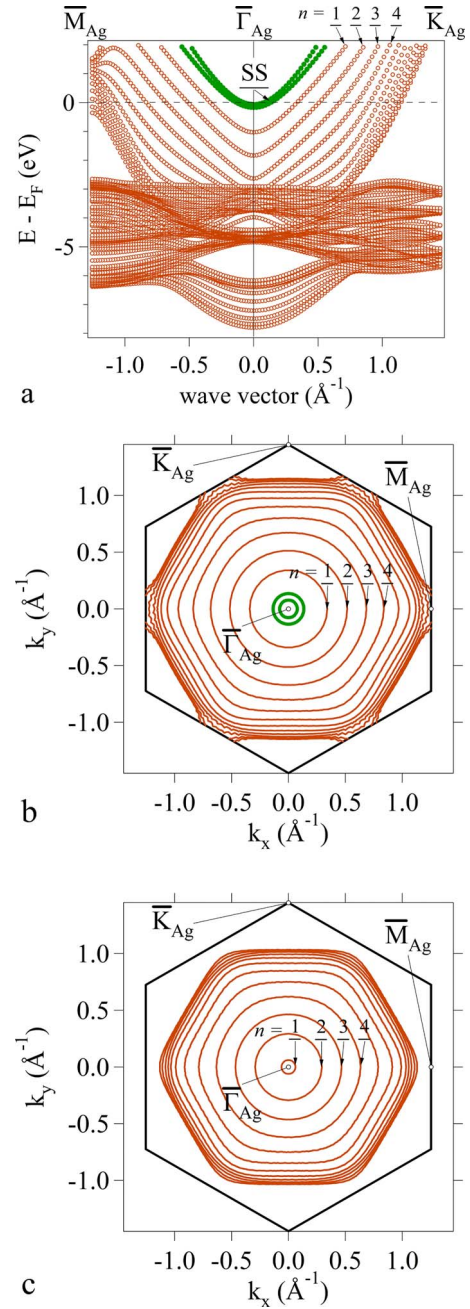

FIG. 1. (Color online) First-principles electronic structure calculations for a free-standing 13 ML Ag(111) film. (a) QW band dispersion along the $\bar{M}$-$\bar{\Gamma}$-$\bar{K}$ line. Panels (b) and (c) display the *sp*-QW contours at E_F and E_F-1 eV, respectively. Due to the interaction of the two surfaces of the film, the surface state splits into an even and odd branch.

spect to the previous one, i.e., with corners lying on the $\bar{\Gamma}$-$\bar{K}$ axes. The $n=2$ state exhibits similar evolution, with corresponding changes in shape occurring at energies closer to E_F. In this case, the energy contour has a ring-like aspect in panel (c) and hexagonal-like shape, with different in-plane orientations, in panels (b) and (d). Notably, the sequence of patterns generated by the $n=3$, 4, and 5 QW states in Fig. 2(e) strikingly contrasts with the monotonic wave vector dependence described in Fig. 1(c).
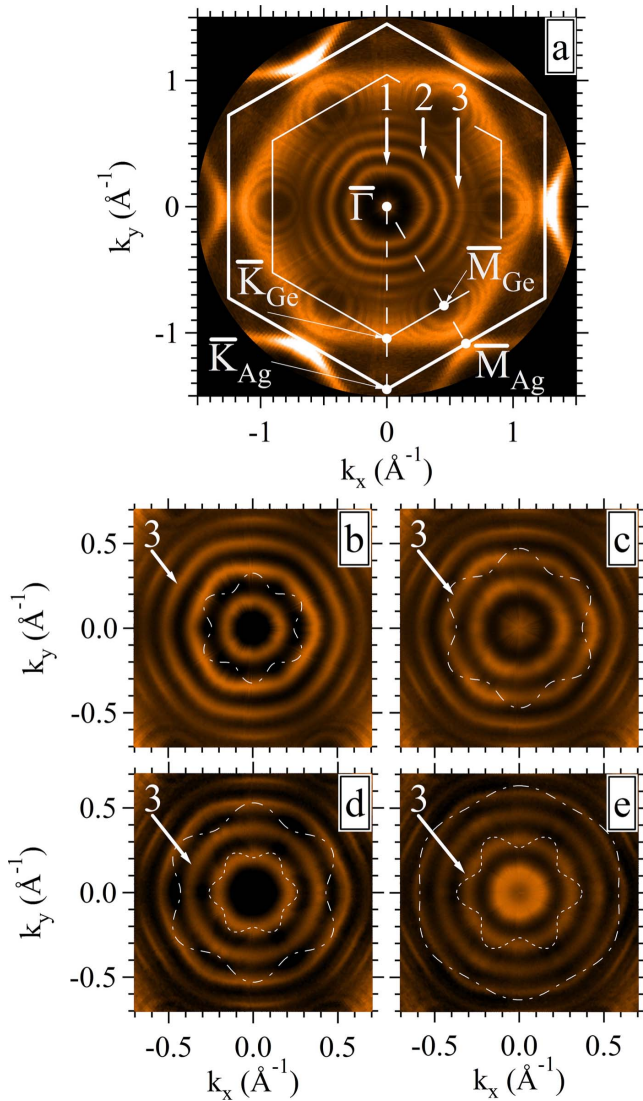
FIG. 2. (Color online) Constant energy cuts through the electronic structure of a 17 ML Ag film grown on Ge(111). The Ag and Ge surface Brillouin zones are displayed with thick and thin continuous lines, respectively. The Fermi surface of the system [panel (a)] displays a series of QW contours with common center at $\bar{\Gamma}$ and multiple ovals surrounding the $\bar{M}_{Ge}$ points. The $n=3$ QW contour appears to be a rounded hexagon at $E_F-0.36$ eV [panel (b)], clearly hexagonal at $E_F-0.66$ eV [panel (c)], round at $E_F-0.81$ eV [panel (d)], and again hexagonal-like at $E_F-1.11$ eV [panel (e)]. The symmetry axes of the hexagonal-like QW contours in panels (c) and (e) are clearly rotated by 30° with respect to each other. Dash-dotted and dotted lines in panels (b)–(e) indicate the onset of the heavy hole and light hole Ge band edges, respectively, as described in the text.

Figure 3 compares theoretical expectations and experimental findings for the energy-momentum dependence of the $n=3$ QW state in the three-dimensional (k_x, k_y, E) space (band bottom view). In absence of a perturbation the state, represented in Fig. 3(a) by a rotational paraboloid with positive aperture, is fully isotropic about the energy axis. When the interaction with the substrate is taken into account, a different band topology emerges [Fig. 3(b)]. The isoenergetic
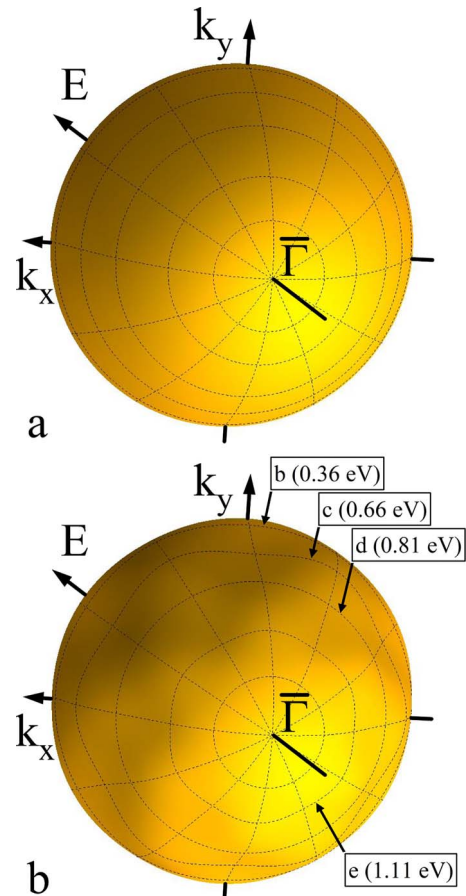

FIG. 3. (Color online) Schematic energy-momentum dispersion relation of a QW state near the center of the surface Brillouin zone in the three-dimensional (k_x, k_y, E) space (band bottom view). (a) Nearly free electron-like case. (b) Interacting case. The complex band topology of the interacting case can be easily evaluated by following the isoenergetic lines labeled (b)–(e), which represent the experimental energy contours observed in the corresponding panels of Fig. 2.

lines labeled with letters (b)–(e), represent the constant energy contours observed experimentally in the corresponding panels of Fig. 2.

In order to explore the origin of the observed behavior we analyze the energy-momentum dependence of the Ag/ Ge(111) electronic structure. Figures 4(a) and 4(b) present intensity maps of the photoemission signal measured along the $\bar{M}$-$\bar{\Gamma}$-$\bar{K}$ line for 9 and 17 ML Ag films, respectively. In both cases the QW bands can be roughly described as parabolas, with multiple breaks interrupting the nearly free electron-like dispersion. By looking more carefully at the data, the gaps seem to open at the crossing points between QW states and sharp bands with downward energy dispersion from $\bar{\Gamma}$, which may remind of the electronic fringes observed in Ag films grown on highly n-doped Si(111).[20] The distribution of these features defines, irrespectively of the film thickness, three sets of curves, displayed in Fig. 4(b) with dashed lines and reported in Fig. 4(c) with full symbols connected by lines. It was already noticed in Ref. 6 that along the $\bar{\Gamma}$-$\bar{K}$ axis the location of the energy gaps closely
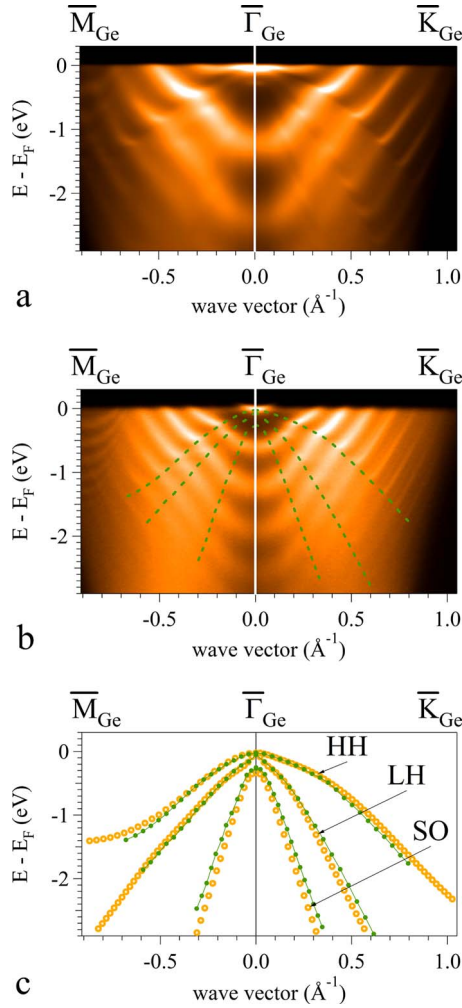
FIG. 4. (Color online) Photoemission intensity maps measured along the $\bar{M}$-$\bar{\Gamma}$-$\bar{K}$ line for (a) 9 and (b) 17 ML Ag films, respectively, displayed within the Ge(111) surface Brillouin zone. Panel (c) reports measured (full symbols connected by lines) and calculated (open symbols) edges of the substrate bands, which are classified as the HH, LH, and SO bands. The measured Ge band edges are also shown in panel (b) as dashed lines.

follows the onset of the substrate bands of different symmetry. In the present study we confirm such relationship and extend its validity in the two-dimensional reciprocal space. Figure 4(c) reports with open symbols the calculated topmost Ge band edges, which are labeled according to the corresponding band symmetry at the $\bar{\Gamma}$ point as the heavy hole (HH), light hole (LH), and split-off (SO) bands. Along the $\bar{\Gamma}$-$\bar{K}$ axis these curves are easily obtained, since they coincide with the Ge bands along the Γ-K bulk direction (if the Ge bulk crystal is set up in an hexagonal lattice). The situation is much more complex along the $\bar{\Gamma}$-$\bar{M}$ axis, for which the analysis of the substrate electronic states has to be extended in the direction perpendicular to the (111) plane. In this case one has to determine the Ge band structure along lines parallel to the Γ-Z direction that project onto the $\bar{\Gamma}$-$\bar{M}$ surface axis. The band onsets are then derived by the envelops of the different sets of calculated bulk bands. From Fig.

4(c) it is evident that along $\bar{\Gamma}$-$\bar{M}$, as well as along $\bar{\Gamma}$-$\bar{K}$, the experimental and calculated results match almost perfectly, thus demonstrating the common origin of the gap openings along different in-plane directions.

The QW state properties seem to depend sensitively on the position relative to the onset of the substrate bands. Sudden variations in the degree of hybridization between Ag and Ge states, which occur at the crossings of the substrate band edges, result in the opening of energy gaps. Changes in the quasiparticle peak width are observed along the QW states across the heavy HH line. Above it, inside the fundamental gap of Ge, the film states are totally confined in two dimensions, while below it the coupling to the substrate wave functions introduces extrinsic peak broadenings. Similar, but less evident, effects are also found across the light LH line. Additionally, the energy dispersion of the QW subbands can be hardly interpolated by a single parabola within the entire wave vector range, besides the effects of distortion associated with the gap openings. The Ge band edges define portions of the energy-momentum space with characteristic phase shifts, which offset unequally the QW branches along the energy axis as a function of the in-plane wave vector.

The above outlined observations allow us to understand in detail the complex behavior described in Fig. 2. The intersection of a constant energy plane with the Ge band edges generates three closed loops, which we can obtain, to a first approximation, as follows. From the curves displayed in Fig. 4(c) we extract the wave vectors along the $\bar{\Gamma}$-$\bar{M}$ and $\bar{\Gamma}$-$\bar{K}$ directions corresponding to a given energy. Then, for each band type we interpolate these values with sinusoids and plot the resulting curves in polar coordinates (dash-dotted lines for the HH band and dotted lines for the LH band in Fig. 2).[21] The anisotropic HH and LH bands give rise to star-like shaped patterns, with protrusions extending toward the $\bar{K}$ and $\bar{M}$ points, respectively. Circles, instead, originate from the SO band (not shown in the pictures). The loops extracted from the HH band cross the $n=2$, 3, 4, and 5 states in panels (b), (c), (d), and (e), respectively, in good correspondence with the observed hexagonal-like distortion. Similarly, the LH-derived loops coincide with the formation of rotated hexagons for the $n=2$ and 3 states in panel (d) and (e), respectively. In absence of edge-induced perturbations the QW contours become nearly circular [see the $n=4$ state in panel (e), for example]. Of course, the symmetry of the QW patterns on constant energy planes is negligibly affected by the effects of hybridization with the isotropic SO band edge.

These considerations can be easily visualized in Fig. 3(b). While moving from the band bottom toward E_F, the phase shift change associated with the crossing of a substrate band edge pushes the QW states to wave vectors larger than expected from a simple parabolic extrapolation [see Figs. 4(a) and 4(b)]. As a consequence, the QW state, which meets the LH edge at deeper energies along $\bar{\Gamma}$-$\bar{K}$ than along $\bar{\Gamma}$-$\bar{M}$, exhibits an hexagonal-like contour with corners lying on the $\bar{\Gamma}$-$\bar{K}$ axes [line (e) in Fig. 3(b)]. This anisotropy tends to fade as the perturbation propagates from the $\bar{\Gamma}$-$\bar{K}$ to the $\bar{\Gamma}$-$\bar{M}$ axes [line(d)]. Similarly, at energies closer to E_F the interaction between the QW state and the HH band edge gives rise to

hexagonally distorted energy contours, with inverted role of the symmetry axes [line (c)]. Finally, a more isotropic dispersion is observed near E_F, where the QW state is decoupled from the Ge electronic bands [line (b)]. The combined effect of phase shift and topology of the substrate band edges fully explains the complex evolution of the QW band patterns as a function of energy and wave vector described in Fig. 2.

For the thinnest Ag layers not only the QW bands appear to be deeply influenced by the interaction with the substrate electronic structure, but also the surface state shows peculiar modifications.[11] Fig. 5 reports the Fermi surface of a 9 ML Ag film grown on Ge(111), where the $n=1$ QW and the surface states are visible. The SS has a rather complex structure, with an extremely intense feature at the zone center, which reminds the Shockley surface state of an Ag(111) crystal, and an hexagonal-like crown at larger in-plane wave vectors. The model developed for the QW states can be used to reproduce the experimental observations. The outer SS contour, in analogy to the $n=1$ QW state appearing at slightly larger in-plane wave vectors, reflects the topology of the HH band edge. The inner subband, instead, displays an hexagonal-like shape, highlighted in the figure by a dashed line, with corners pointing toward the $\bar{K}$ points. This distortion is likely to derive from the coupling to the anisotropic LH band edge. As already observed in Ref. 11, the coupling between surface and substrate wave function, which perturbs the otherwise nearly free electron-like surface state, rapidly vanishes with increasing the film thickness.

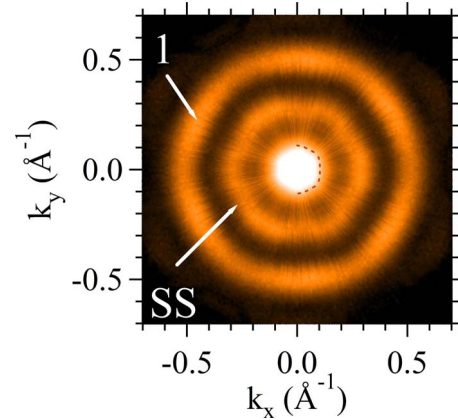In conclusion, in this paper we have described by angle-

FIG. 5. (Color online) Fermi surface of a 9 ML Ag film grown on Ge(111). The dotted line surrounding the bright (saturated) feature at the zone center highlights its hexagonal-like aspect.

resolved photoemission and with the support of first-principles calculations the complex energy and wave-vector dependence of the band patterns generated by the QW and surface states in Ag layers on Ge(111). An unusual sequence of ring-like and hexagonal-like constant energy contours with different in-plane orientations is shown to manifest the interrelation occurring between substrate and film band topologies.

[1] T.-C. Chiang, Surf. Sci. Rep. **39**, 181 (2000).

[2] J. E. Ortega and F. J. Himpsel, Phys. Rev. Lett. **69**, 844 (1992); J. E. Ortega, F. J. Himpsel, G. J. Mankey, and R. F. Willis, Phys. Rev. B **47**, 1540 (1993).

[3] L. Aballe, C. Rogero, P. Kratzer, S. Gokhale, and K. Horn, Phys. Rev. Lett. **87**, 156801 (2001).

[4] C. Koitzsch, C. Battaglia, F. Clerc, L. Despont, M. G. Garnier, and P. Aebi, Phys. Rev. Lett. **95**, 126401 (2005).

[5] A. M. Shikin and O. Rader, Phys. Rev. B **76**, 073407 (2007).

[6] I. Matsuda, T. Ohta, and H. W. Yeom, Phys. Rev. B **65**, 085327 (2002).

[7] S.-J. Tang, L. Basile, T. Miller, and T.-C. Chiang, Phys. Rev. Lett. **93**, 216804 (2004).

[8] S.-J. Tang, Wen-Kai Chang, Yu-Mei Chiu, Hsin-Yi Chen, Cheng-Maw Cheng, Ku-Ding Tsuei, T. Miller, and T.-C. Chiang, Phys. Rev. B **78**, 245407 (2008).

[9] Eli Rotenberg, Y. Z. Wu, J. M. An, M. A. Van Hove, A. Canning, L. W. Wang, and Z. Q. Qiu, Phys. Rev. B **73**, 075426 (2006).

[10] D. V. Vyalikh, Yu. Kucherenko, F. Schiller, M. Holder, A. Kade, S. L. Molodtsov, and C. Laubschat, Phys. Rev. B **76**, 153406 (2007).

[11] S.-J. Tang, T. Miller, and T.-C. Chiang, Phys. Rev. Lett. **96**, 036802 (2006).

[12] S.-J. Tang, Y.-R. Lee, S.-L. Chang, T. Miller, and T.-C. Chiang, Phys. Rev. Lett. **96**, 216803 (2006).

[13] P. Moras, L. Ferrari, C. Spezzani, S. Gardonio, M. Ležaić, Ph. Mavropoulos, S. Blügel, and C. Carbone, Phys. Rev. Lett. **97**, 206802 (2006).

[14] Y. Liu, N. J. Speer, S.-J. Tang, T. Miller, and T.-C. Chiang, Phys. Rev. B **78**, 035443 (2008).

[15] L. Basile, H. Hong, P. Czoschke, and T.-C. Chiang, Appl. Phys. Lett. **84**, 4995 (2004).

[16] E. Wimmer, H. Krakauer, M. Weinert, and A. J. Freeman, Phys. Rev. B **24**, 864 (1981).

[17] For a program description see http://www.flapw.de.

[18] C. Li, A. J. Freeman, H. J. F. Jansen, and C. L. Fu, Phys. Rev. B **42**, 5433 (1990).

[19] G. Cubiotti, Yu. Kucherenko, A. Yaresko, A. Perlov, and V. Antonov, J. Phys.: Condens. Matter **11**, 2265 (1999).

[20] N. J. Speer, S.-J. Tang, T. Miller, and T.-C. Chiang, Science **314**, 804 (2006).

[21] This procedure is justified by the fact that, for symmetry reasons, the band onsets along the $\bar{\Gamma}$-$\bar{M}$ and $\bar{\Gamma}$-$\bar{K}$ directions must be extremal (either maxima or minima).